



Seismic behaviors of steel plate shear wall structures with construction details and materials



Wang Meng^{a,*}, Yang Weiguo^a, Shi Yongjiu^b, Xu Jian^c

^a School of Civil Engineering, Beijing Jiaotong University, Beijing 100044, China

^b Department of Civil Engineering, Tsinghua University, Beijing 100084, China

^c China Southwest Architectural Design and Research Institute Corp. Ltd, Chengdu 610081, China

ARTICLE INFO

Article history:

Received 3 May 2014

Accepted 8 January 2015

Available online 23 February 2015

Keywords:

Steel plate shear wall structure

Structural construction detail

Low yield point steel

T type stiffened ribs

Finite element method (FEM)

Hysteretic behavior

ABSTRACT

In order to have a systematic and comprehensive comparison of seismic behaviors of steel plate shear wall structures with different construction details, a numerical method was proposed, which was proved accurately to predict the performance of structures with published quasi-static tests. Then, eight typical steel shear wall models with different structural construction details were established. Also an advanced stiffened low yield point steel plate shear wall was proposed to avoid excessive out-of-plane deformation. The seismic behaviors of above nine shear wall models were fully compared and analyzed, and key issues, such as energy-dissipating capacity, ductility, out-of-plane deformation and the effect of tension field on the columns were discussed in depth. The results showed that: in high-intensity seismic area, load-carrying capacity, hysteretic behaviors, failure modes, seismic ductility and economic performance should be taken into account comprehensively to choose the appropriate form of steel plate shear wall structure; the proposed low yield point steel plate shear wall with T type stiffened ribs could most effectively improve the energy dissipation capacity and ductility, and lessen the impact of tension field on the columns, besides, it had better load-carrying capacity and smallest out-of-plane deformation. This method provided a good way for improving the seismic behaviors of steel shear wall structures.

© 2015 Elsevier Ltd. All rights reserved.

1. Introduction

Recently, Steel frame–steel plate shear wall structure is a research hotspot for its excellent performance on resisting lateral deformation, so it has already been used in many high-rise steel buildings. Due to large steel consumption, low utilization efficiency of material and poor welding performance of thick steel plate shear wall, thin steel plate shear wall structures are paid more attention in current studies. This kind of structure has larger height to thickness ratio λ of infill panel ($\lambda > 150$), therefore, when a small horizontal force is applied, the buckling of steel panel occurs earlier with larger out-of-plane deformation. And then, the tension fields of thin infill plate are formed, making the structure continue to resist the horizontal force. These tension fields will be transmitted directly to the frame columns, resulting in a greater impact on frame columns [1,2]. In order to improve the seismic behaviors of thin steel plate shear wall structures, research works are mainly focused on two aspects. On one hand, the design principle of “strong frame, weak wall” is proposed in the view of performance matching. Currently, many scholars have suggested various structural constructions of shear walls based on this principle, including shear panel with

openings [3,4], shear panel slotted at both sides [5] and shear panel with vertical slits [6–8], as shown in Fig. 1. On the other hand, the buckling of steel infill plate in advance will lead to larger out-of-plane deformation with loud sounds, which may adversely affect the comfort demands and using of requirements. Some researchers have presented several stiffened steel plate shear wall structures (for example, cross-stiffened, groined stiffened and diagonal stiffened steel plate shear walls [8–11], as shown in Fig. 1) and buckling-restrained measures [12] to delay and lessen the buckling behaviors of panels. Some other researchers also proposed low yield point steel plate shear wall structures [3,13] based on new materials, indicating that this kind of structure had better ductility and energy dissipation capacity [14,15] due to the better seismic behaviors of low yield point steel [16,17]. All the works above have significant effects on improving the energy dissipation capacity of steel plate shear walls, and reducing the adverse impacts of buckling on structures.

In this field of researches, most of the studies, however, focused on one or a few construction details. No systematic and comprehensive comparison of seismic behaviors of steel plate shear walls with different construction details has been implemented. Due to high costs of tests, comprehensive comparison is difficult to carry out only by means of test method, and also some seismic indexes cannot be obtained by experiments (e.g., fracture tendency and the effect of tension field on

* Corresponding author. Tel.: +86 13811718116; fax: +86 10 51684947.
E-mail address: wangmeng1117@gmail.com (M. Wang).

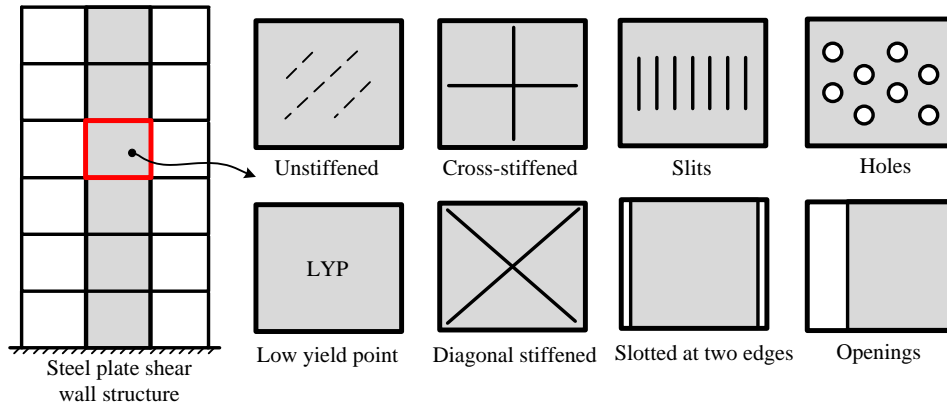


Fig. 1. Steel plate shear wall structures with different structural construction details.

the columns). Therefore, the numerical simulations are widely used currently. The more accurate finite element model for parametric analysis is particularly important. However, due to the severe non-linear behaviors of reciprocating two-way tension fields, the constantly changing out-of-plane deformation and the zero or even negative stiffness phenomena, the accurate numerical simulation of thin steel plate shear wall structures subjected to cyclic loading is difficult to achieve. Furthermore, the responses of materials under cyclic loading and monotonic loading are quite different [18]. The traditional method cannot accurately predict the cyclic behaviors, local buckling phenomena and pinching phenomena. Therefore, a more efficient and accurate finite element method should be proposed for thin steel plate shear wall structures.

In this study, many improved construction details of steel plate shear walls were summarized. Firstly, the finite element models of thin steel plate shear wall under cyclic loading patterns were established using ABAQUS software. The computing platform, element selection, meshing, the initial imperfection and steel cyclic constitutive models were introduced in detail. Geometric nonlinearity and material nonlinearity were considered adequately. The results of numerical simulation were compared with typical experimental results. The proposed method was proved to accurately simulate and predict the seismic behaviors, including capacity and stiffness degradation caused by out-of-plane deformation, pinch phenomena of curves, failure modes and fracture positions, which provided a strong tool for carrying out further analysis. Then, based on the verified finite element method, eight typical steel shear wall models with different structural construction details and unstiffened low yield point steel shear wall model were established within common sizes, and their load-carrying capacity, hysteretic behavior, degradation characteristics, fracture index, failure modes, energy-dissipating capacity, especially ductility, out-of-plane deformation and the effect of tension field on the columns were deeply analyzed. Besides, to lessen the out-of-plane buckling phenomenon and improve

the load-carrying capacity of low yield point steel plate shear wall, an advanced stiffened low yield point steel plate shear wall was proposed, and its seismic behaviors were also compared with all others above. Finally, a direct suggestion was given for engineers to choose proper construction details according to the specific demands of actual projects. It was expected to provide a reference for engineering applications.

2. Finite element analysis

In order to study the behaviors of the steel plate shear wall structures, an efficient and accurate finite element method should be obtained. All parts of models are presented in more detail as follows.

2.1. Model description

A typical steel plate shear wall structure generally consists of edge beams, edge columns, infill panel, beam-to-column connections, and fish plates, as shown in Fig. 2. It was proved in reference [19] that the fish plate could be neglected in finite element model, which would not affect the simulated results. Both H-shaped frame and infill panel are modeled in ABAQUS with shell element S4R, to avoid shear locking phenomenon. In order to accurately simulate the plate buckling, initial defect should be imposed on the panel by rewriting the inp file. The process of imposing initial defect is achieved by using Command “imperfection” to modify the coordinates of nodes. Reference [1] drew a conclusion that residual stress had little effect on behaviors of steel plate shear wall, which could be ignored. Therefore, the residual stress will not be considered in the finite element modeling.

The boundary conditions and loading patterns are in accordance with typical tests. The loading process contains two steps. Firstly, the vertical loads are applied on the top of edge columns to simulate the axial forces, and the impact of second-order effect is taken into account.

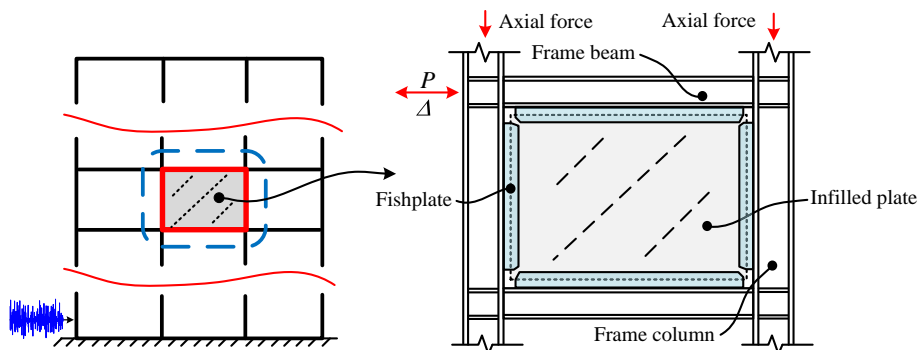


Fig. 2. Typical element of steel plate shear wall.

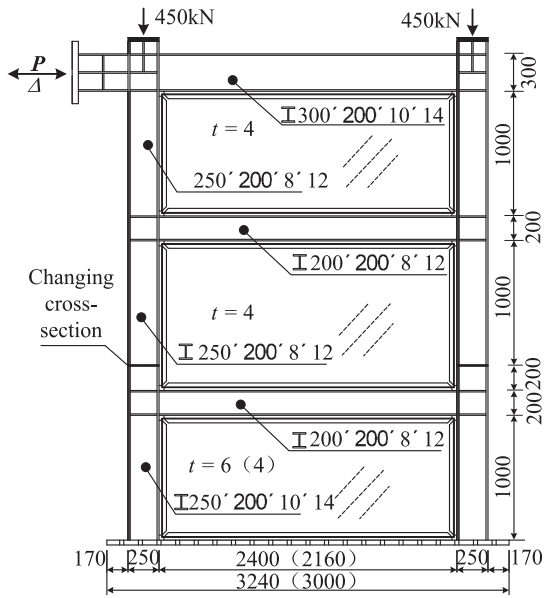


Fig. 3. Specimen details of Xu Jian et al. (mm).

Secondly, the horizontal load P or displacement Δ is imposed on edge beam to simulate the horizontal seismic loading.

2.2. Material modeling

Reference [18] showed that the stress–strain curve of steel under cyclic loading was quite different from the one under monotonic loading, and the traditional material constitutive model with monotonic loading curve was difficult to meet the calculation accuracy. Therefore, the cyclic constitutive model should be used, which can accurately simulate the cyclic hardening, buckling, cumulative damage and degradation phenomena of structures subjected to cyclic loading patterns [20]. Therefore, the constitutive model proposed by Chaboche [21,22] is adopted, which is parameterized in ABAQUS (HARDENING = COMBINED model) [23].

2.3. Computing platform

Since the main object of study is the thin steel plate shear wall under cyclic loadings, strong nonlinear behaviors should be simulated, including apparent buckling (infill panel buckling and column and beam local buckling), out-of-plane deformation, as well as the mutations of the tension strips of steel plate. Therefore, the analyses are conducted in ABAQUS 6.10/explicit module [23]. This method treats the static problem as a dynamic process and uses the central difference method for gradual integration of structural motion equations, which is appropriate for solving highly nonlinear problems. The structure density is needed, and an appropriate loading speed is selected as 0.5 every step. For static test, the loading rate was relatively slower, therefore, it has little effect on the calculation results. Due to the obvious local buckling phenomena, the mesh sizes would affect the calculative results. Based on the

sensitivity analysis of meshing, the number of 20 is determined for meshing within the range of tension stripes, which could satisfy the required calculative accuracy. Besides, structural meshes should be used. The time step size is calculated automatically in ABAQUS, according to the minimum mesh size of models.

3. Verifications of numerical analysis

In order to verify the finite element method, typical quasi-static tests were selected, including the tests of Xu et al. [24], Vian et al. [3], Li et al. [8,11] and Chen et al. [13].

3.1. Tests of Xu Jian et al.

Four 1:3 unstiffened steel plate shear wall specimens with three floors were designed in reference [24], and specimens TM2–TM4 were selected in this paper. The detailed dimensions of specimens are shown in Fig. 3, and the parameters in brackets are the specific values for specimen TM3, which are different from other specimens. The material of infill panel is Q235B steel and the edge columns and beams are made of steel Q345B. The cyclic constitutive model proposed in Part 2 is adopted. The yield strengths are selected according to the material tests in reference [24], and the related cyclic hardening parameters are from Table 1. The initial defect of out-of-plane is applied based on the measured data in reference [24]. Test loading method is shown in Fig. 3. During the horizontal cyclic loading process, the ratio of axial compression stress to strength maintains 0.2.

The load–displacement curves (P – Δ) and typical failure modes calculated by finite element model and tests are compared in Fig. 4. The numerical simulations are basically the same as experimental results, indicating that the numerical method could accurately predict the cumulative damage, strength degradation, pinching phenomena, deformation developing process, local buckling of panels and columns, and crossed tension strips of steel plate shear walls.

3.2. Tests of Vian et al.

The experimental studies on seismic performance of new-type steel plate shear wall structures (shear walls with equipment holes according to the practical requirements) were conducted in reference [3]. Specimen sizes and mesh details are shown in Fig. 5. Specimen S2 is a solid steel plate without holes. There are several circular holes in infill panel of specimen P. Specimen CR has two openings (1/4 circular arc with radius 500 mm) at the corners of the panel. The stiffeners are set at the edge of arc openings with 160 mm width and 19 mm thickness, as shown in Fig. 5(b). Edge frames are made of A572 steel, and the yield strength is 345 N/mm². The yield strength of infill panel is 165 N/mm². The related cyclic hardening parameters refer to Table 1. The first-order buckling mode is used for geometric initial defect. The specific value is 1/500 height of steel plate according to the recommendation in reference [24]. Cyclic loading patterns are applied at the middle of beam until the component is completely destroyed.

The calculated load–displacement curves (P – Δ) and the predicted failure modes are accordant with experimental results in Fig. 6, indicating that the numerical method could simulate the hysteretic behaviors. Because of obvious out-of-plane deformation of specimen CR (Fig. 6(c)),

Table 1
Hardening parameters of materials.

	Q_{∞} (N/mm ²)	b	C_1 (N/mm ²)	γ_1	C_2 (N/mm ²)	γ_2	C_3 (N/mm ²)	γ_3	C_4 (N/mm ²)	γ_4
Q345B/Q235B	21	1.2	7993	175	6773	116	2854	34	1450	29
High strength steel	16	1.2	4924	154	3101	120	2730	31	1450	26
Low yield strength steel	100	8.0	8000	400	1200	130	2730	100		

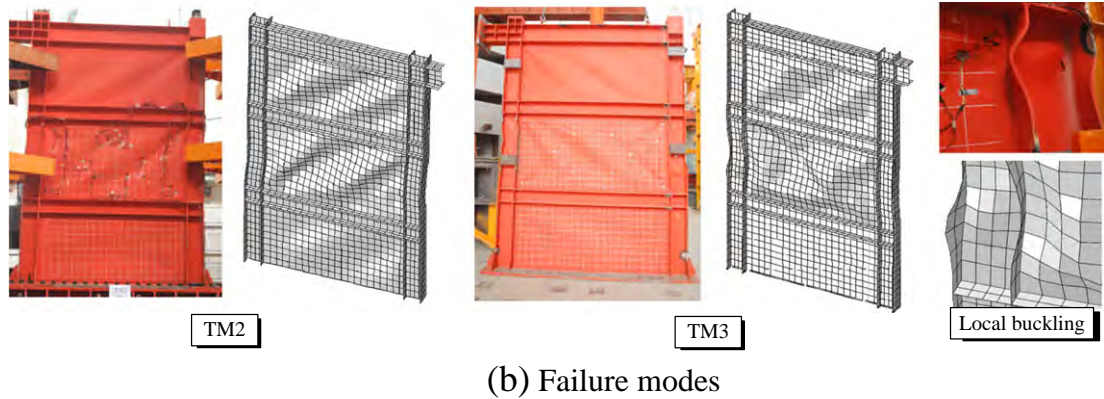
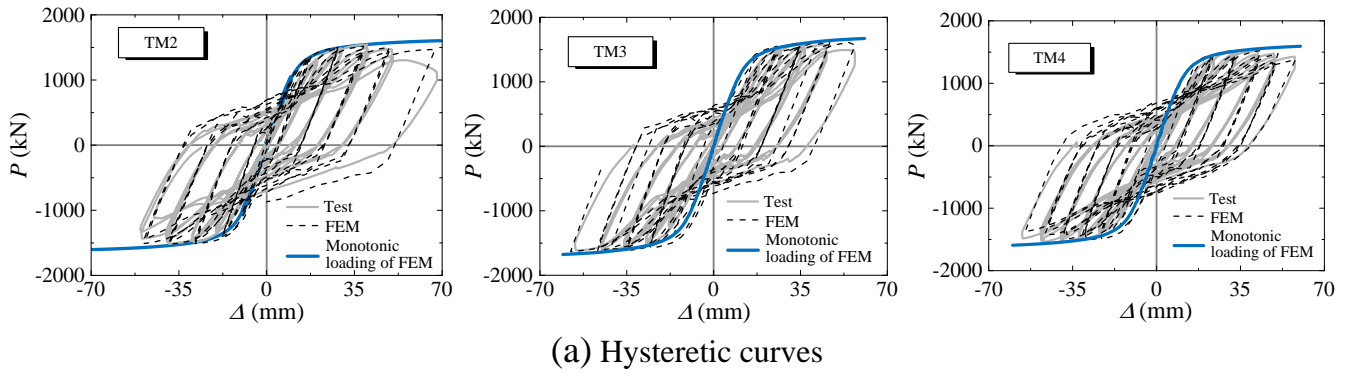
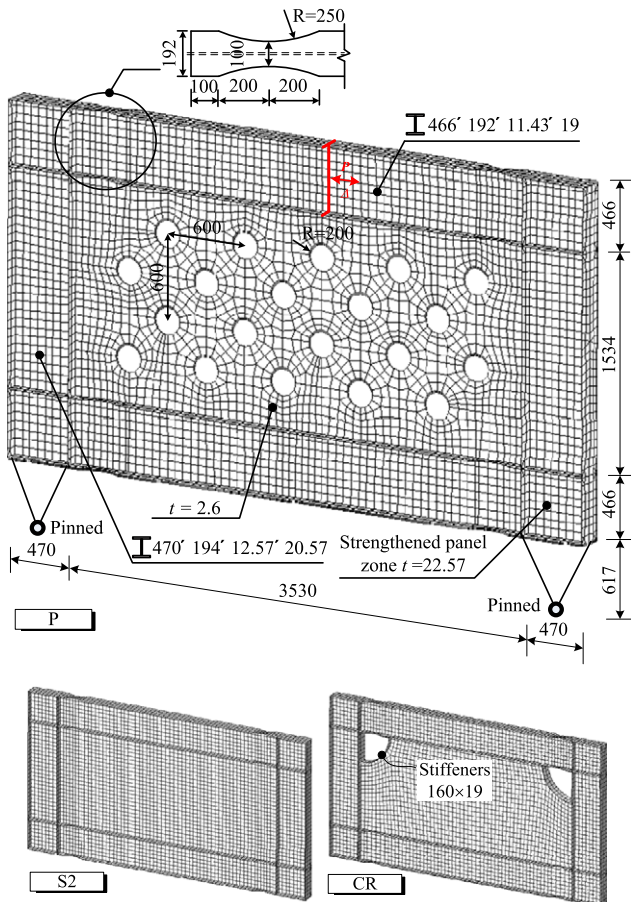


Fig. 4. The comparison of test and FEM of Xu Jian et al.



the load-carrying capacity decreases significantly, and this phenomenon could also be well simulated by the proposed method.

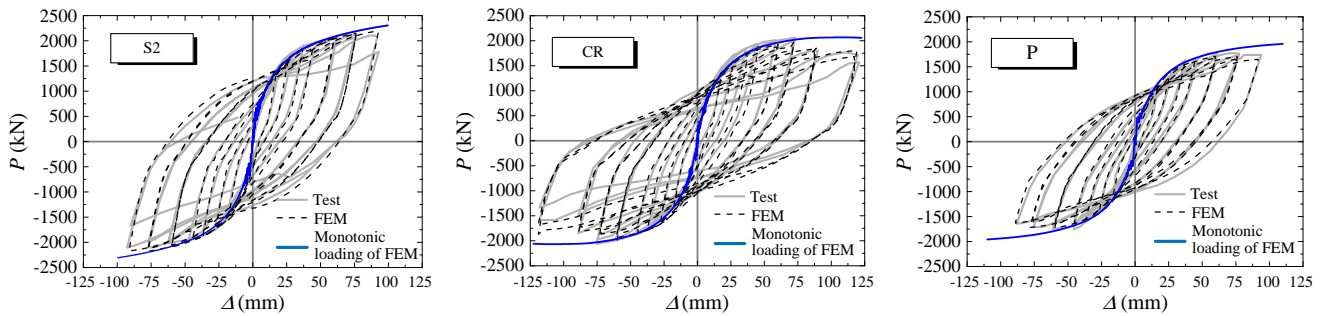
3.3. Tests of Li et al.

The cyclic loading tests of steel plate shear wall structures with different construction details were conducted in references [8] and [11]. The sections of edge frames are the same, while the forms of infill panels are different, including unstiffened steel plate shear wall (H), shear wall with slits (HD1), shear wall with openings (HD2), cross-stiffened shear wall (HS1) and diagonal stiffened shear wall (HS2). The detailed dimensions and meshes are shown in Fig. 7. The width and length of the vertical slits on specimen HD1 are respectively 5 mm and 240 mm, and the spacing of slits is 75 mm. The out-of-plane initial defects of shear wall are determined according to references [8] and [11]. The material of edge frames and infill panel is Q235B steel. The basic material test data are according to references, and the cyclic constitutive model proposed in Part 2 is adopted (Table 1). During the horizontal cyclic loading process, the axial forces on specimens maintain 400 kN.

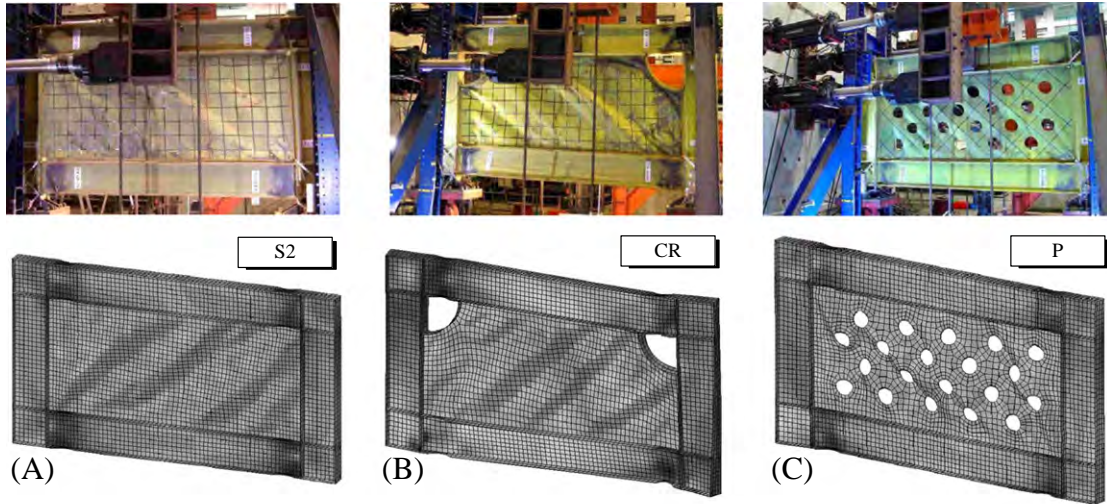
The calculated load–displacement curves ($P-\Delta$) and experimental results are well compared in Fig. 8. Typical failure modes are compared in Fig. 9. Most specimens have local buckling of the columns, out-of-plane deformation and buckling of stiffeners. The slit strips of HD1 are deformed badly with serious bending. The simulated overall and local failure modes are consistent with actual situations.

3.4. Tests of Chen et al.

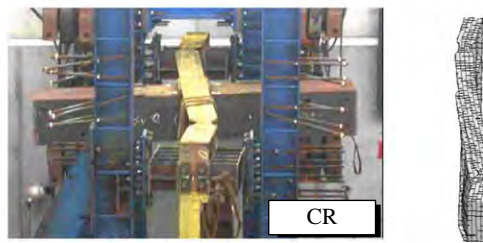
The purpose of reference [13] was to study the seismic behaviors of low yield point steel plate shear wall under cyclic loading patterns. LYP100 is used for shear panel. Edge frames are made of A572 steel. The yield strengths are referred to Ref. [13], and the cyclic constitutive



(a) Hysteretic curves



(b) Failure modes



(c) Out-of-plane deformation

Fig. 6. The comparison of test and FEM of Vian et al.

model proposed in Part 2 is adopted (Table 1). The details of specimens No. 3 and No. 4 and meshes of finite element model are shown in Fig. 10(a).

The calculated hysteretic curves (P - θ) and tests are basically the same in Fig. 10(c) and (d). The cyclic skeleton curves are higher than monotonic curves, which are caused by cyclic hardening behaviors of LYP steel material. The comparison results show that the numerical method could accurately simulate the cyclic behaviors of the low yield steel plate shear wall structures.

3.5. Prediction of maximum capacity

The load-carrying capacities of mentioned eleven specimens are predicted. Comparisons of experimental and numerical results are shown in Fig. 11(b). $P_{\max,ex}$ is the maximum imposed load of experimental results, $P_{\max,an}$ is the maximum imposed load of numerical results and P_y is the yield load of experimental results (the yield strength and yield

displacement are defined in Fig. 11(a)). The deviation from the solid line indicates the error of the numerical results. The error defined by Eq. (1) is 3.3%, revealing that the finite element method is reliable for simulating load-carrying capacity of specimens.

$$\text{Error} = \frac{1}{n} \sum_{i=1}^n \frac{|P_{\max,ex} - P_{\max,an}|}{P_{\max,ex}} \quad (1)$$

3.6. Prediction of fracture tendency

The fracture tendency can be predicted by equivalent plastic strain (PEEQ), which is described as a cumulative variable and a monotonically increasing function (Eq. (2)). $\bar{\varepsilon}^{pl}$ is calculated in Eq. (3). This index represents the local ductility and fracture tendency of steel (ABAQUS 6.10) [23].

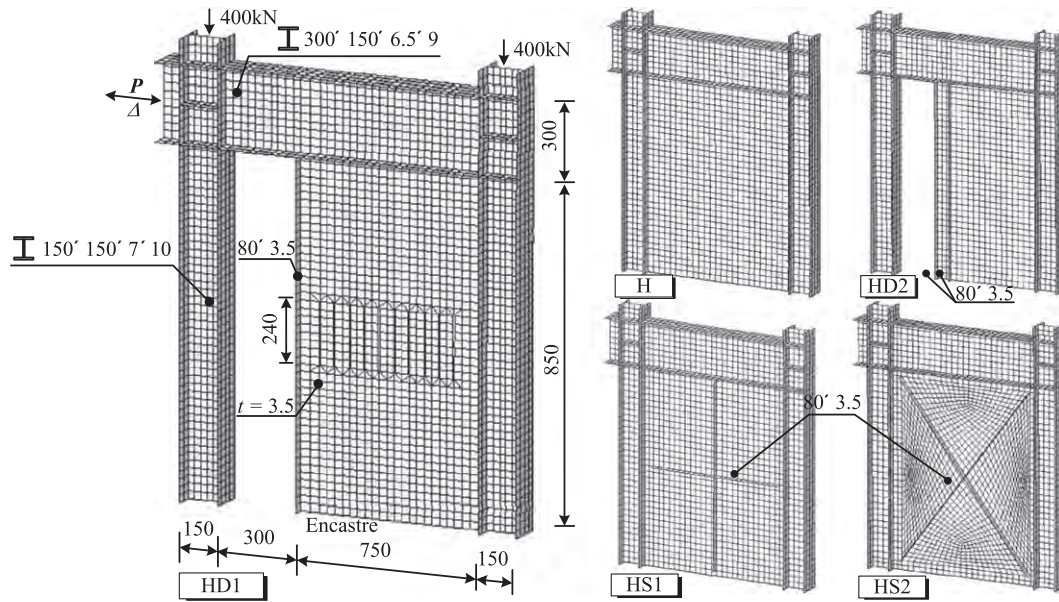


Fig. 7. Specimen details and meshing of Li et al. (mm).

$$PEEQ = \dot{\varepsilon}^{\text{pl}} \Big|_0 + \int_0^t \dot{\varepsilon}^{\text{pl}} dt \quad (2)$$

$$\dot{\varepsilon}^{\text{pl}} = \sqrt{\frac{2}{3}} \dot{\varepsilon}^{\text{pl}} : \dot{\varepsilon}^{\text{pl}} \quad (3)$$

where $\dot{\varepsilon}^{\text{pl}}$ is the rate of plastic flow, $\dot{\varepsilon}^{\text{pl}}$ is the equivalent plastic strain rate and $\dot{\varepsilon}^{\text{pl}} \Big|_0$ is the initial equivalent plastic strain rate.

From Fig. 12, the positions of the maximum PEEQ are consistent with the ones of actual fractures in tests, indicating that the numerical method can determine the probable fracture locations. Therefore, in practical engineering, based on the calculated results, appropriate measures can be used to avoid fracture in advance.

In summary, the proposed three-dimensional finite element method could simulate the hysteretic behaviors of steel plate shear wall structure more accurately, and could also give a more precise description of the whole process under cyclic loading. It provides a powerful tool for further analyses of steel plate shear wall structures with different construction details.

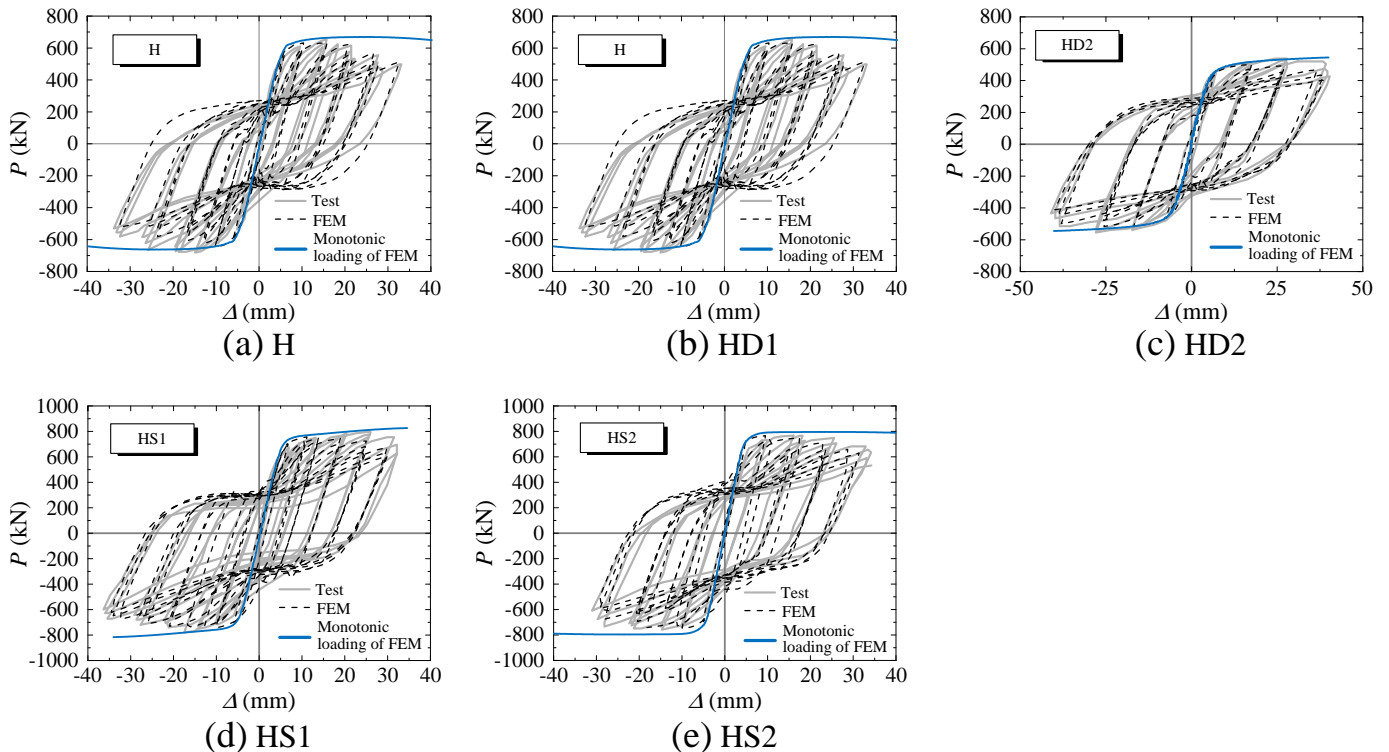


Fig. 8. Hysteretic curve comparison of test and FEM of Li et al.

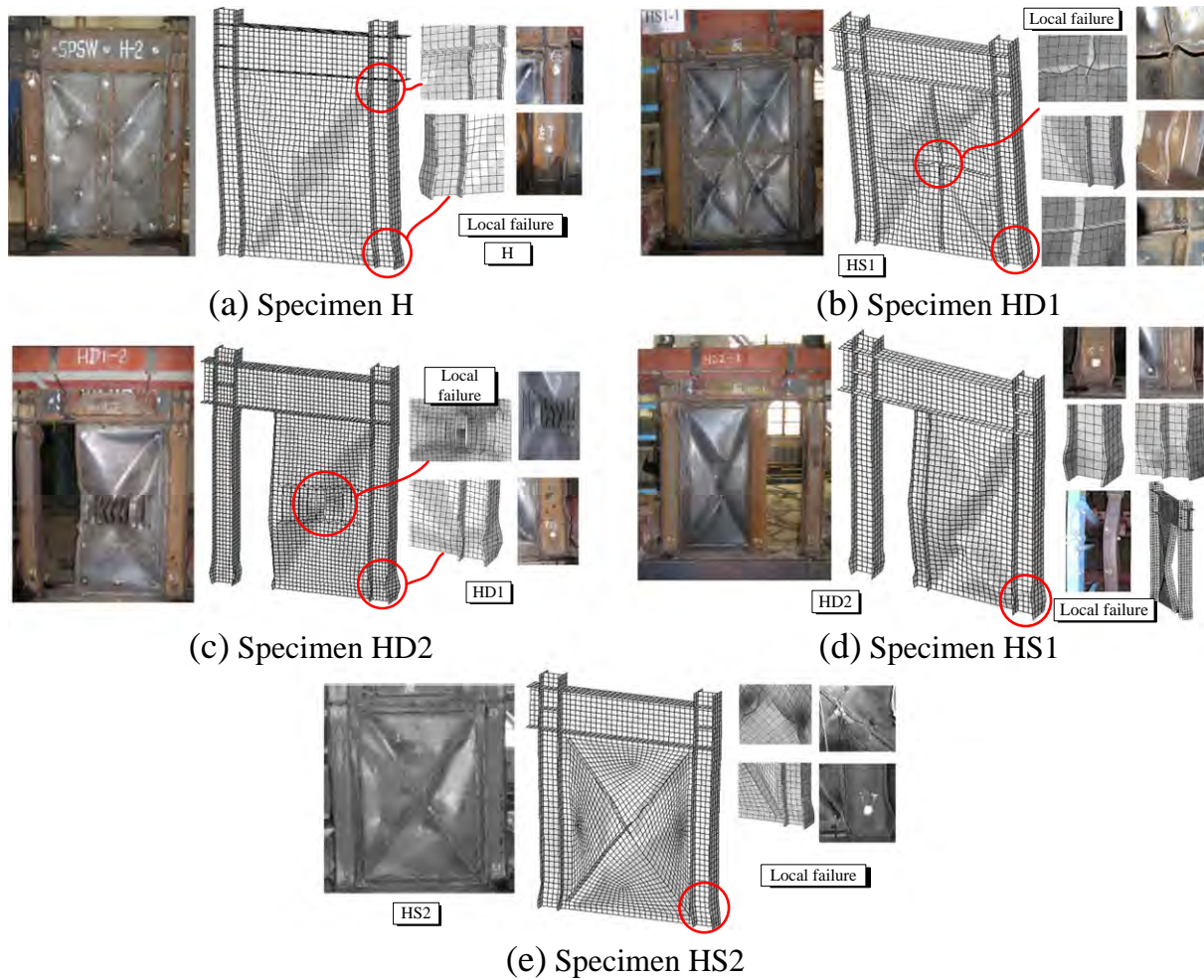


Fig. 9. Failure mode comparison of test and FEM of Li et al.

4. Parameters of steel plate shear wall structures with different construction details and materials

The construction details and materials have great effect on behaviors of steel plate shear wall structures. The construction details mentioned below are most widely used in engineering projects. In order to gain a direct understanding for engineers to choose proper construction details in terms of specific situations, steel plate shear wall structures with different construction details and materials are studied.

4.1. Typical steel plate shear wall structures with different construction details

The finite element models of steel plate shear wall structures with typical construction details are established, and comparative analyses are carried out with (1) standard unstiffened steel plate shear wall in Table 2. Considering the practical engineering applications, the span to depth ratio of thin steel plate shear wall is $L/h = 1.0\text{--}2.0$, and the height to thickness ratio is around $\lambda = 200\text{--}400$ [24]. In order to investigate the seismic behaviors of steel plate shear wall with large ratio of height to thickness, the span to depth ratio is determined as 1.25, and the height to thickness ratio is determined as 350. The index of edge column stiffness was proposed by American and Canadian specifications based on the developing degree of tension fields [25,26]. The stiffness should meet the requirement of Eq. (4).

$$\omega_h = 0.7h_s \left[\frac{t_f}{2L_s I_c} \right]^{0.25} \quad (4)$$

$$\omega_h \leq 2.5$$

where h_s and L_s are respectively the center distances of edge beams and edge columns; I_c is the inertia moment of edge column; t_f is the thickness of infill wall; and h is the height of infill wall. ω_h of specimen (1) is 2.2, satisfying the requirement for edge column stiffness. On the other hand, the influences of the column deformation on structures could be studied.

All the specimens have the same sizes of edge frames and the same thickness of infill steel panels with different construction details. The shear regions of beam-to-column connections are strengthened as 14 mm. The detailed dimensions of models are shown in Fig. 13. The specific types and numbers are shown in Table 2. (1) Standard specimen (SW-STA) is a solid unstiffened steel plate shear wall. (2) Slotted steel plate shear wall (SW-CF): the infill panel is not connected to the edge columns with 50 mm gaps. (3) Steel plate shear wall with slits (SW-SF): there are several slits in infill panel. The width and length of the vertical slit are respectively 5 mm and 500 mm, and the spacing of slits is 100 mm. The proportion of slit arrangement is consistent with reference [7]. (4) Cross-stiffened steel plate shear wall (SW-SR): the double-faced cross stiffeners are welded on the infill panel, and the stiffener sizes are designed and determined according to reference [8]. (5) Diagonal stiffened steel plate shear wall (SW-CR): the double-faced diagonal stiffeners are welded on the infill panel with the same

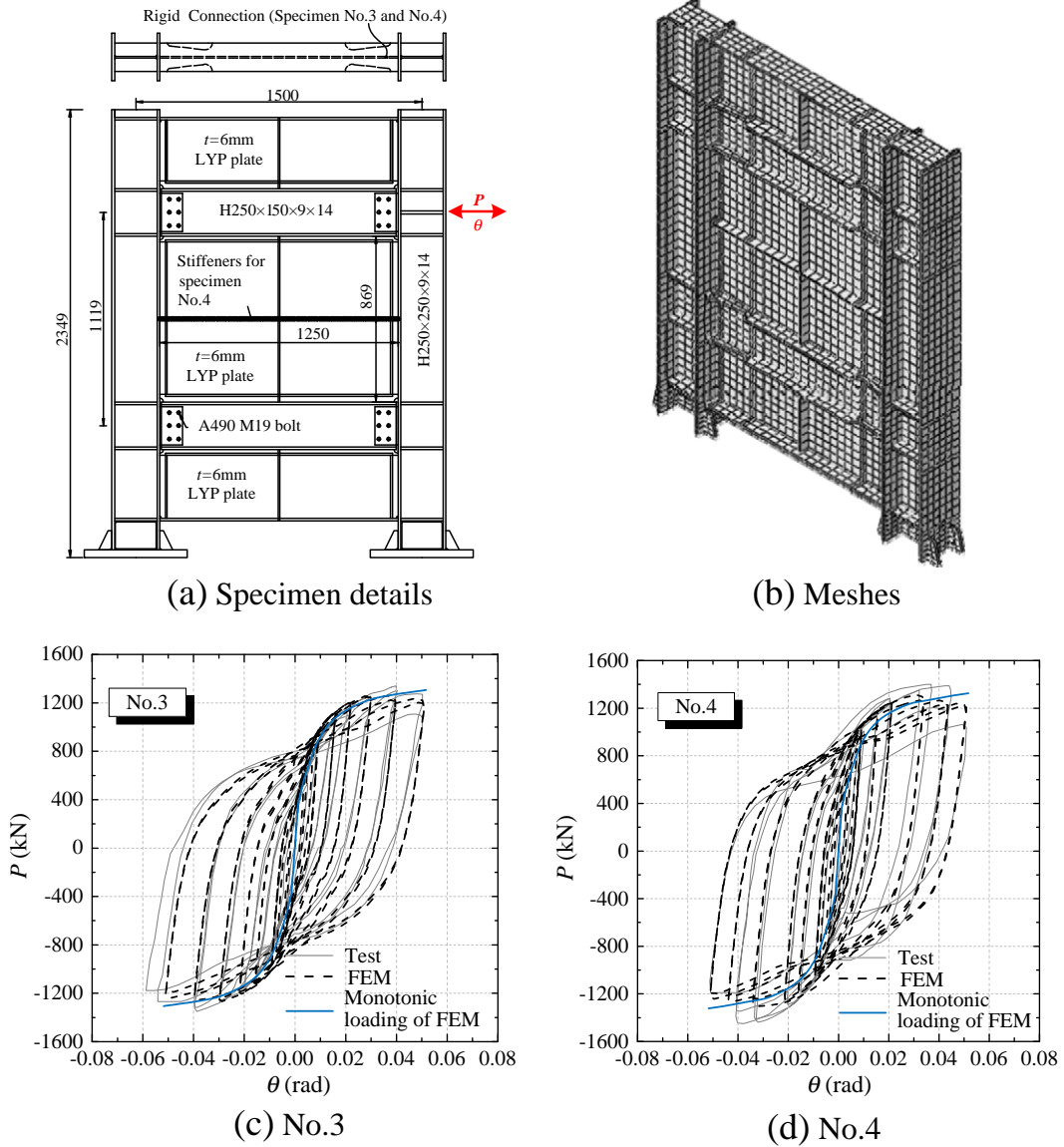


Fig. 10. The comparison of test and FEM of Chen et al.

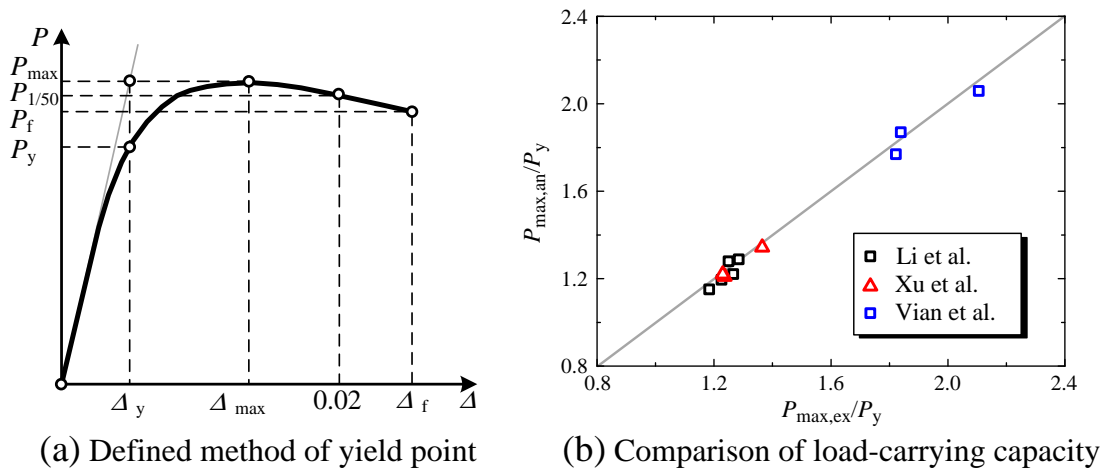


Fig. 11. Prediction of load-carrying capacity.

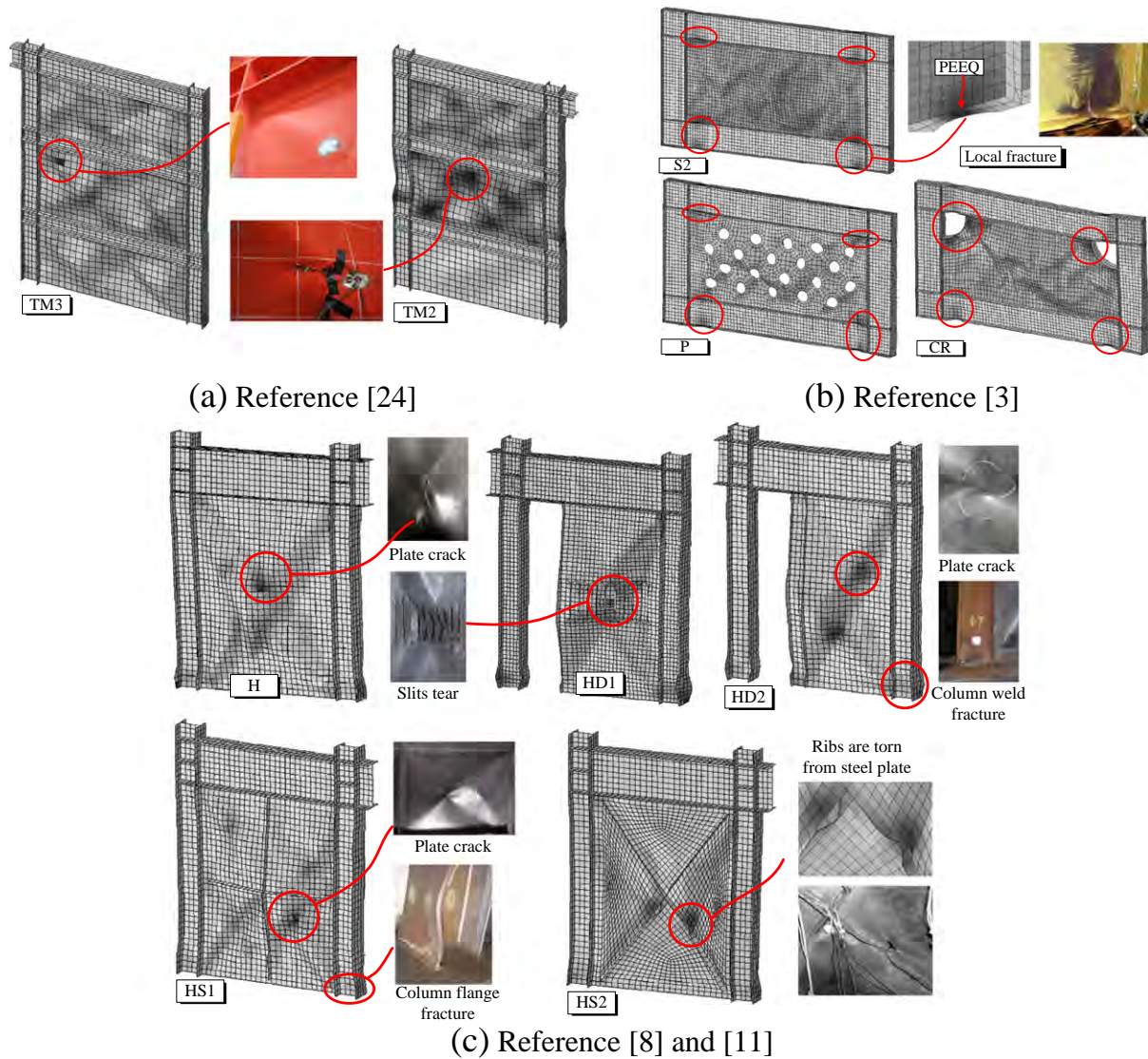


Fig. 12. Prediction of fracture properties.

cross-section of cross stiffeners. (6) Steel plate shear walls with openings-I (SW-H1) and (7) -II (SW-H2): the size of holes is determined according to reference [3] with a diameter of 200 mm.

4.2. Low yield point steel plate shear wall structures

In order to study the effect of infill panel material on seismic performance of shear wall structure, low yield point steel LYP100 is used for infill panel ((8) low yield point steel plate shear wall (SW-LYP)). The hysteretic curves of low yield point steel are plumper than normal steel [27] with good energy dissipation capacity and ductility, and the yield to strength ratio is only 0.3–0.4 with high load-carrying capacity potential [13,16]. Special material will inevitably lead to the obvious different behaviors of steel plate shear wall structures from ordinary ones. However, due to the lower yield strength, the lateral stiffness of low yield point steel plate shear wall is less than ordinary one in case of the same thickness, resulting in earlier out-of-plane deformation, louder noises, and pinching phenomenon of hysteresis curve under cyclic loadings. Therefore, based on better solderability of low yield point steel [12], author proposes an advanced double-sided stiffened rib (T type stiffened ribs in Fig. 14). This kind of stiffened rib has greater bending stiffness and higher stiffened efficiency, and can effectively improve the performance of low yield point steel plate shear wall. Meanwhile,

this method can inhibit buckling to some extent, reduce the out-of-plane deformation, and ensure the ductility and energy-dissipating capacity of low yield point steel.

For comparative purposes, the detailed dimensions of low yield point steel plate shear walls are the same as standard steel plate shear wall. One kind of the proposed T type rib stiffened low yield point steel plate shear wall is also compared with other shear wall structures

Table 2

Parameter illustration of steel plate shear wall structures with different structural constructions.

Influence factors	Types	Numbers
Standard steel plate shear wall	(1) The standard specimen	SW-STA
The effect of slits	(2) Slotted steel plate shear wall at two edges	SW-CF
	(3) Steel plate shear wall with slits	SW-SF
The effect of stiffeners	(4) Cross-stiffened steel plate shear wall	SW-SR
	(5) Diagonal stiffened steel plate shear wall	SW-CR
The effect of holes	(6) Steel plate shear wall with openings I	SW-H1
	(7) Steel plate shear wall with openings II	SW-H2
The effect of material	(8) Low yield point steel plate shear wall	SW-LYP
	(9) T type rib stiffened low yield point steel plate shear wall	SW-T-LYP

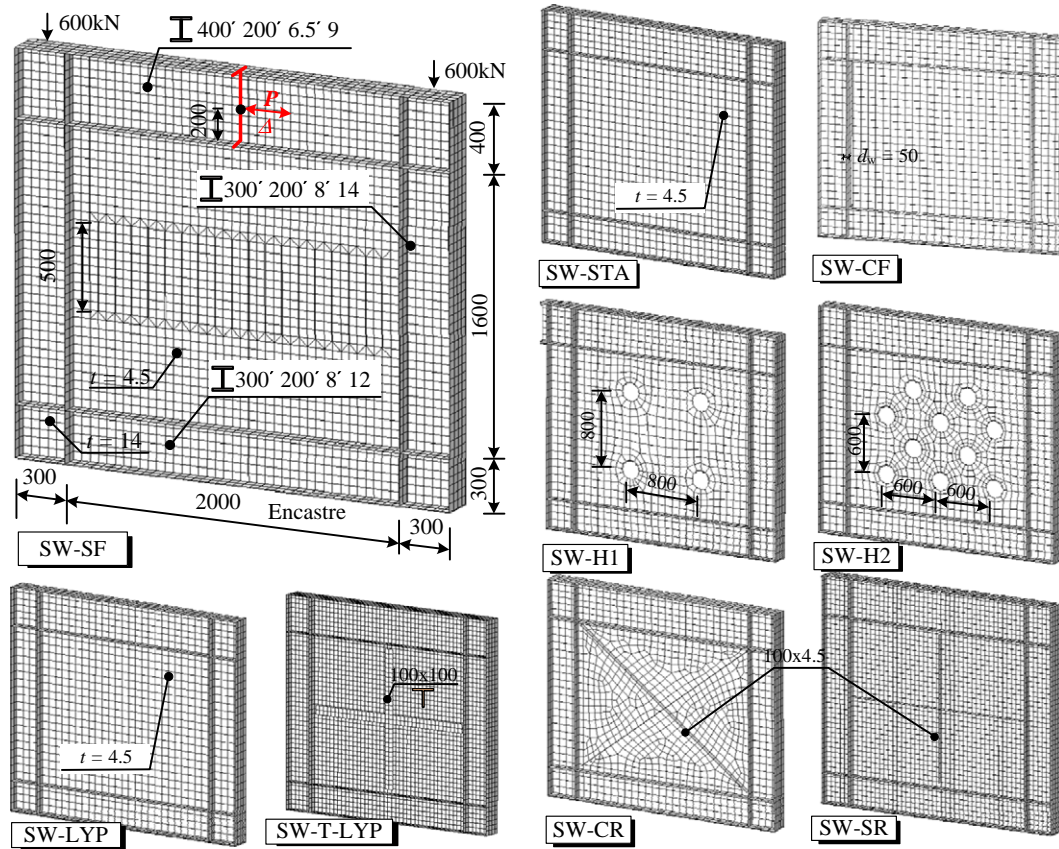


Fig. 13. Detailed dimensions and finite element models of steel plate shear wall structures (mm).

(called (9) SW-T-LYP in Table 1), and the height and thickness of T type stiffened rib are the same as stiffened steel plate shear wall. The finite element models of all shear wall structures are shown in Fig. 13.

4.3. Material characteristics and constraint condition

Based on the principle of “strong frame, weak wall”, the yield strength of edge frame is 380 MPa, and 240 MPa for infill panel of normal steel. The nominal yield strength of low yield point steel is 100 MPa, and its isotropic hardening phenomenon is more obvious than normal steel as the increasing of hysteretic loops [13]. The cyclic constitutive parameters are determined according to references [18] and [27] (Table 3). The bottoms of specimens are fixed. The nodes of connections are restrained to prevent out-of-plane instability. The specific value of initial defect is 1/500 height of steel plate. The ratio of axial compression stress to strength maintains 0.2. All the specimens are displacement-controlled with the same loading patterns (Fig. 15). The definition of inter-story drift angle is $\theta = \Delta/H$, where Δ is the imposed

displacement, and H is the height of storey. The inter-story drift angle 0.02 rad is the collapse limit of Code for Seismic Design of Buildings in China [28]. The maximum imposed displacement is 60 mm (θ is 0.03 rad) to investigate the behaviors under strong earthquakes.

5. Seismic behaviors of steel plate shear wall structures with different construction details

5.1. Comparison of hysteretic behaviors

Due to the cyclic hardening constitutive model of materials, the monotonic loading curves will appear below the cyclic skeleton curves before degradation occurs. Therefore, in order to study the degradation phenomena caused by cyclic loading, the determined method of the equivalent monotonic curves in Fig. 16 is that cyclic displacements are imposed before 20 mm, and then monotonic displacement is imposed until 60 mm. It can be seen from Figs. 16 and 17 that as the numbers of hysteretic loops are increasing, the differences of hysteretic

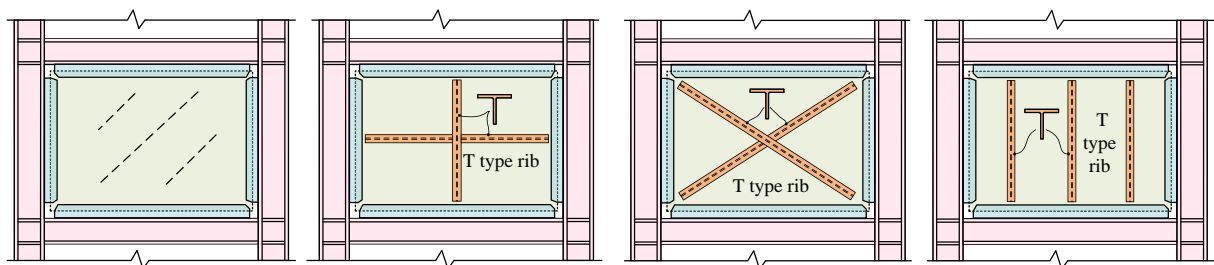


Fig. 14. T type rib stiffened low yield point steel plate shear wall.

Table 3
Parameters of specimen materials.

Type	σ_{f0} (MPa)	Q_{∞} (MPa)	b_{iso}	$C_{kin,1}$ (MPa)	γ_1	$C_{kin,2}$ (MPa)	γ_2	$C_{kin,3}$ (MPa)	γ_3	$C_{kin,4}$ (MPa)	γ_4
Column and beam	380	16	1.1	4924	154	3101	120	2730	31	1450	26
Wall	240	21	1.2	4924	154	3101	120	2730	31	1450	26
Wall with low yield strength steel	100	100	8.0	8000	400	1200	130	2730	100		

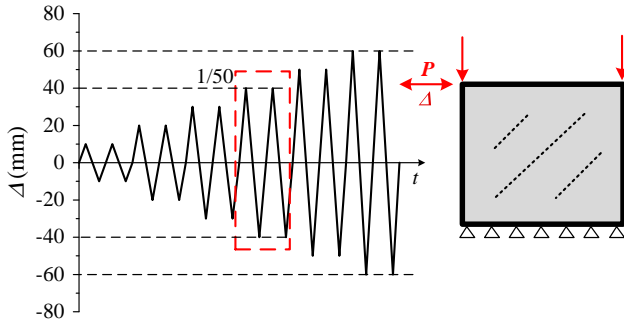


Fig. 15. Loading patterns.

curves and equivalent monotonic curves become more obvious. It indicates that plastic deformation accumulation observably aggravates the out-of-plane deformation, the local buckling of columns and the

formation of tension field, resulting in strength and stiffness degradation subjected to cyclic loadings.

Because of the reciprocating out-of-plane deformation of steel panel, pinching phenomena occur in hysteretic curves with gradually forming two-way tension strips. The deformation is continuously recovering, and the length of zero stiffness stage in curve is growing. The pinching degrees of steel plate shear wall structure with different construction details are not consistent. Due to material properties of low yield point steel, the hysteretic curves of low yield point steel plate are relatively fuller with less degradation, especially SW-T-LYP with effective restraints. The deformation modes of SW-CF and SW-SF are changed, so the hysteretic loops are fuller. The curve of SW-SF is different from others, because of bending deformation of steel strips between slits. Due to limited stiffness of stiffeners on SW-SR and SW-CR, the out-of-plane deformation of steel panel and local buckling of stiffeners appear in succession, leading to obvious pinching and degradation phenomena of hysteretic curves. The curves of SW-H1 and SW-H2 also have pinching phenomena.

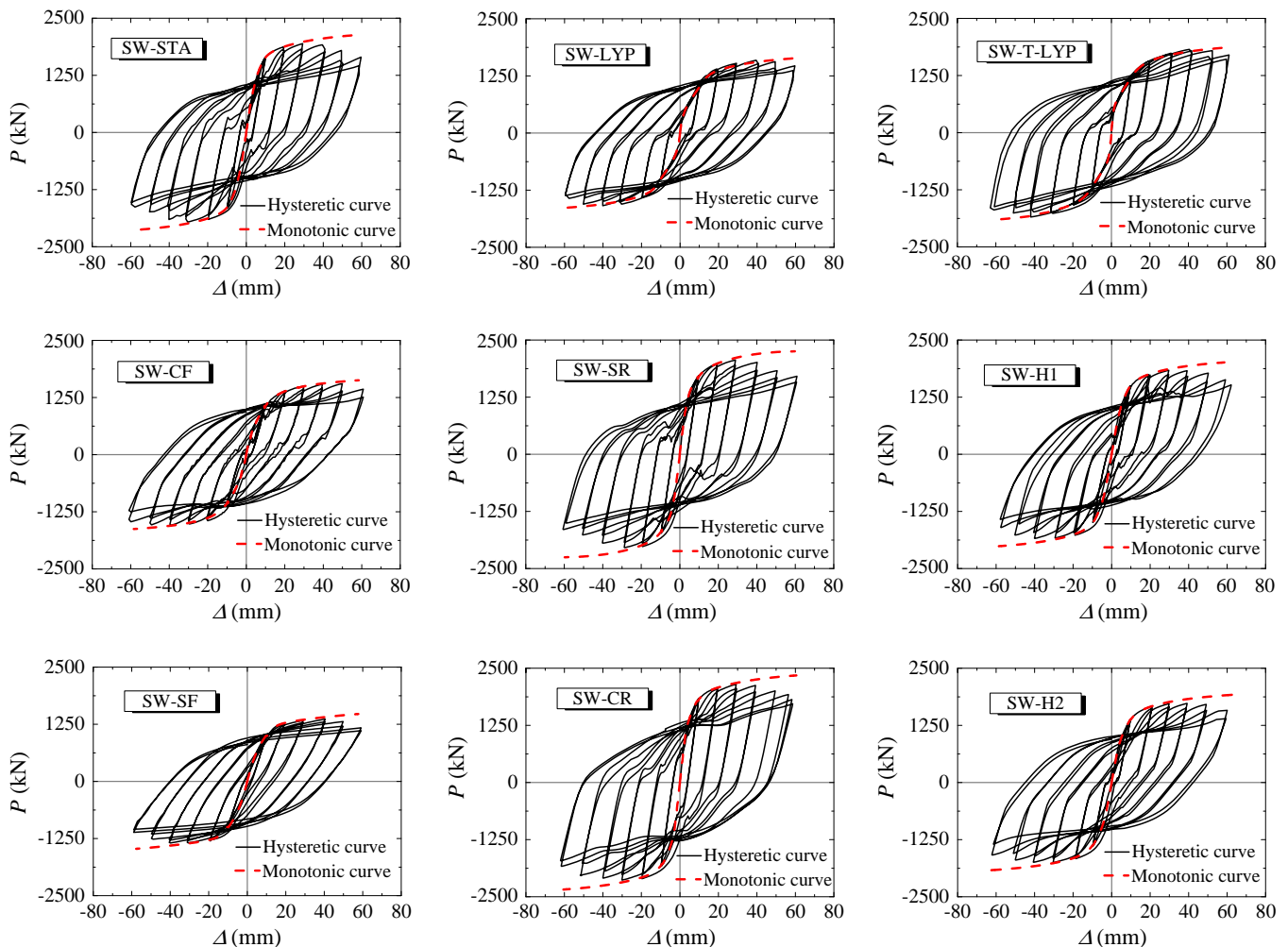


Fig. 16. Comparison of hysteretic curves.

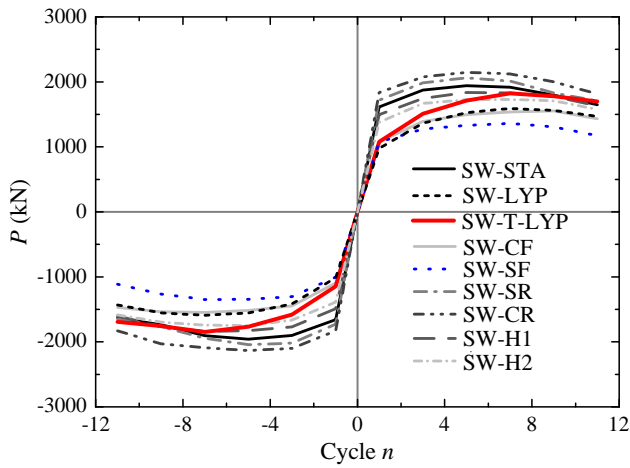


Fig. 17. Comparison of cyclic skeleton curves.

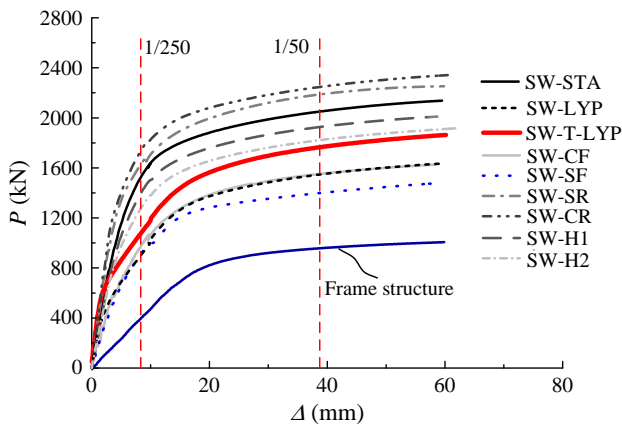


Fig. 18. Comparison of monotonic curves.

5.2. Comparison of load-carrying capacity

The out-of-plane deformations of thin steel plate shear walls occur earlier. The lateral stiffness is decreased with the horizontal displacement increasing, showing a strong nonlinear feature, as shown in Fig. 18. The initial stiffness K_i is defined as the secant stiffness of position with imposed displacement of 1.2 mm. The equivalent stiffness K_{si} is the secant stiffness of position with 1/250 inter-story drift angle (1/250 is the equivalent elastic drift limit of seismic code [28]). The monotonic load-carrying capacity of frame structure is 1006.28 kN, less than half of the ultimate capacity of standard shear wall structure. The initial lateral stiffness is 48.99 kN/mm, less than 1/6 of standard shear wall

structure. The above comparison data indicate that the steel panels have great effect on improving the load-carrying capacity of frame structures.

Seen from Figs. 17 and 18 and Table 4, the strength and stiffness of shear walls with various details are quite different. Though the steel yield strength of LYP is only one third of normal one, the load-carrying capacity decreases by only about 20%, indicating that the material utilization is higher. The initial stiffness K_i of SW-LYP is 92% of SW-STA (the probable reason is that some local positions have already yielded (for instance, the corners of the panel wall)), however, the equivalent stiffness K_{si} is only 61% of SW-STA, revealing that the stiffness decreases quickly due to yielding and buckling. Due to the effective stiffening, the load-carrying capacity of SW-T-LYP is much higher than SW-LYP, especially initial stiffness to make up for the disadvantages of SW-LYP; and the peak strength under cyclic loading is only a little less than SW-STA, as shown in Fig. 17 and Table 4. The strength and stiffness of SW-CF and SW-SF are much less than SW-STA, indicating that the tension fields are changed, greatly affecting the load-carrying capacity. The steel consumption of SW-SR increases by 11%, while the strength is enhanced by about 5%, the initial stiffness K_i about 36% and the equivalent stiffness K_{si} about 11%. The steel consumption of SW-CR increases by 16%, while the strength is improved by about 10%, the initial stiffness K_i about 36% and the equivalent stiffness K_{si} about 15%. The above data indicate that the stiffeners have more significant effect on initial stiffness. From the comparison data of SW-H1 and SW-H2 in Table 4, the effects of openings on strength are proportional to opening areas, but the effects on stiffness are slightly larger. In summary, the construction details have some influences on performances of shear wall structures, however, the carrying capacities increase greatly comparing with pure frame.

5.3. Comparison of strength degradation

Degradation is related to plastic deformation accumulation of structures, out-of-plane deformation of steel plate, and local buckling of columns. The strength degradation index is defined as $\Delta P/P_{mi}$, where $\Delta P = P_k - P_{mi}$. P_{mi} is the reaction force at each cyclic amplitude displacement and P_k is the equivalent monotonic reaction force at the corresponding displacement. The shear wall structures with different construction details have different degradation starting positions, degradation degrees, degradation developing paths and degradation stability, as shown in Fig. 19. From the hysteretic curves in Fig. 16, due to the strength decreases under the same imposed displacement, the degradation curves are obtained respectively according to odd and even loading cycles. Red dash rectangles in Fig. 19 are the degradation degrees at inter-story drift angle of 1/50, and the values are shown in Table 5. The final degradation degrees are also compared in Table 6 (inter-story drift angle is 1/30).

It can be seen from Fig. 19(a) that SW-T-LYP and SW-LYP have stable performance without severe strength degradation, and the degradation starting positions are much later than SW-STA. In Fig. 19(b), the early

Table 4
Comparison of load-carrying capacity behaviors.

Type	P_{cui}/kN	P_{cui}/P_{cu1}	P_{mui}/kN	P_{mui}/P_{mu1}	K_i kN/mm	K_i/K_1	K_{si} kN/mm	K_{si}/K_{s1}	K_{si}/K_i
SW-STA	1943.21	1.00	2135.34	1.00	280.70	1.00	192.01	1.00	0.68
SW-LYP	1592.47	0.82	1635.74	0.77	257.25	0.92	116.23	0.61	0.45
SW-T-LYP	1846.02	0.95	1863.23	0.87	370.03	1.32	138.44	0.72	0.37
SW-CF	1553.27	0.80	1627.47	0.76	168.23	0.60	119.46	0.62	0.71
SW-SF	1331.24	0.69	1475.39	0.69	155.43	0.55	113.42	0.59	0.73
SW-SR	2063.34	1.06	2252.21	1.05	357.84	1.27	208.12	1.08	0.58
SW-CR	2148.09	1.11	2336.68	1.09	383.02	1.36	220.85	1.15	0.58
SW-H1	1837.71	0.95	2010.37	0.94	238.95	0.85	175.70	0.92	0.74
SW-H2	1730.22	0.89	1916.84	0.90	241.19	0.86	160.29	0.83	0.66

Note: P_{cui} is the peak value of cyclic skeleton curve. P_{mui} is the peak value of monotonic curve.

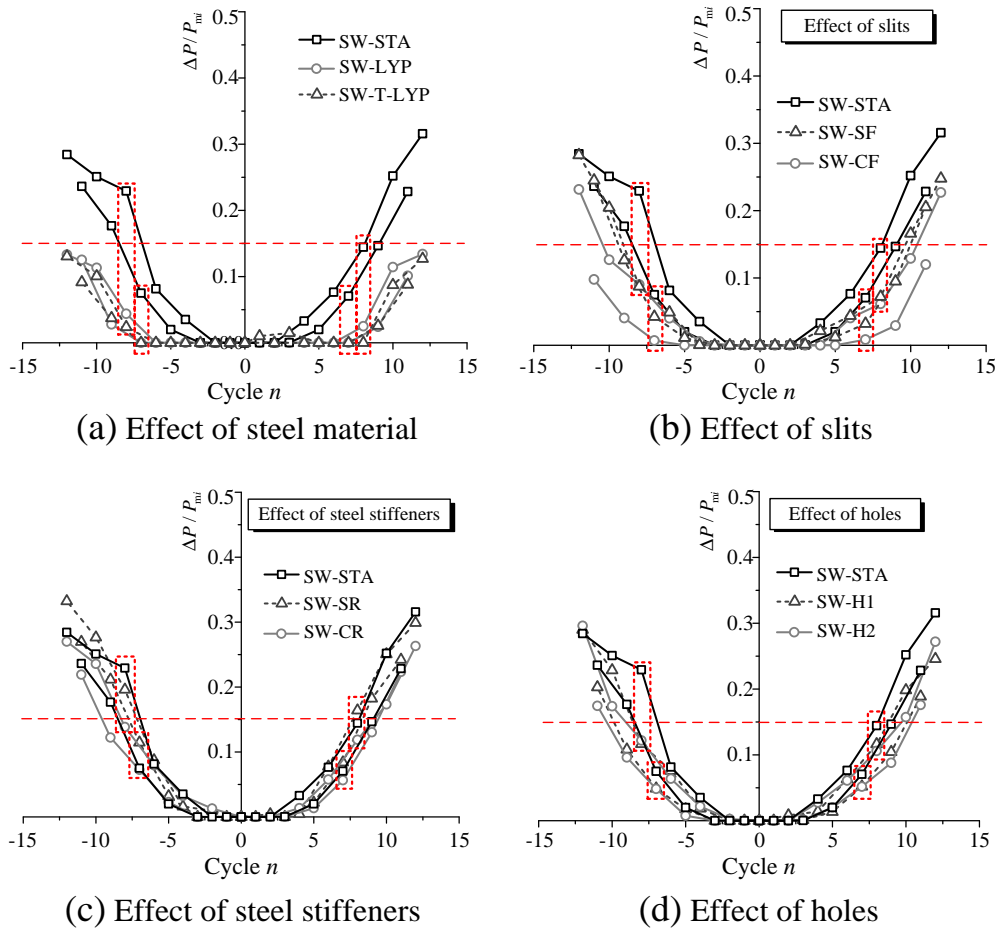


Fig. 19. Comparison of strength degradation.

degradations of SW-SF are less than SW-STA, however, the degradation rates increase because of severe deformations of steel strips between slits. SW-CF has more stable performance of degradation. In Fig. 19(c), at 1/50 position, the degradation of SW-STA is relatively more serious than the others, while SW-CR is relatively small. At the final position, the degradation values of SW-SR are the largest due to the severe buckling of stiffeners, reducing the restraint effect. In Fig. 19(d), the degradation degrees of SW-H1 and SW-H2 are less than SW-STA at the position of 1/50, while the final degradation values of three structures are

similar. According to the requirements of seismic code [28] in defining the position of degradation by 15% as failure point (horizontal dash line in Fig. 19), the later the intersection points appear, the relatively better the ductility of shear wall structures is. The strength degradations of SW-T-LYP, SW-LYP, SW-CF, SW-SF, SW-H1 and SW-H2 are less than 15% at 1/50 position with good ductility. Comparing with SW-STA, the failure points of other structures occurred later, indicating that proper construction changes can improve the ductility of structures.

Table 5
Degraded characteristics of steel plate shear wall structures (1/50 position).

Type	$(\frac{\Delta P}{P_m})_{\max}^{+,e}$	$(\frac{\Delta P}{P_m})_{\max}^{-,e}$	$(\frac{\Delta P}{P_m})_{\max}^{+,o}$	$(\frac{\Delta P}{P_m})_{\max}^{-,o}$
SW-STA	0.14	0.23	0.07	0.07
SW-LYP	0.02	0.04	0.00	0.00
SW-T-LYP	0.00	0.02	0.00	0.00
SW-CF	0.06	0.09	0.01	0.01
SW-SF	0.07	0.09	0.03	0.04
SW-SR	0.16	0.20	0.08	0.11
SW-CR	0.11	0.13	0.06	0.07
SW-H1	0.12	0.12	0.05	0.04
SW-H2	0.10	0.12	0.05	0.04

Note: $(\frac{\Delta P}{P_m})_{\max}^{+,e}$ is the maximum strength degradation of even cycle in positive direction.
 $(\frac{\Delta P}{P_m})_{\max}^{-,e}$ is the maximum strength degradation of even cycle in negative direction.
 $(\frac{\Delta P}{P_m})_{\max}^{+,o}$ is the maximum strength degradation of odd cycle in positive direction.
 $(\frac{\Delta P}{P_m})_{\max}^{-,o}$ is the maximum strength degradation of odd cycle in negative direction.

Table 6
Degraded characteristics of steel plate shear wall structures (final position).

Type	$(\frac{\Delta P}{P_m})_{\max}^{+,e}$	$(\frac{\Delta P}{P_m})_{\max}^{-,e}$	$(\frac{\Delta P}{P_m})_{\max}^{+,o}$	$(\frac{\Delta P}{P_m})_{\max}^{-,o}$
SW-STA	0.31	0.28	0.22	0.23
SW-LYP	0.13	0.13	0.1	0.12
SW-T-LYP	0.22	0.23	0.11	0.09
SW-CF	0.24	0.28	0.20	0.24
SW-SF	0.29	0.33	0.24	0.26
SW-SR	0.26	0.27	0.22	0.21
SW-CR	0.24	0.29	0.18	0.20
SW-H1	0.27	0.29	0.17	0.17
SW-H2	0.31	0.28	0.22	0.23

Note: $(\frac{\Delta P}{P_m})_{\max}^{+,e}$ is the maximum strength degradation of even cycle in positive direction.
 $(\frac{\Delta P}{P_m})_{\max}^{-,e}$ is the maximum strength degradation of even cycle in negative direction.
 $(\frac{\Delta P}{P_m})_{\max}^{+,o}$ is the maximum strength degradation of odd cycle in positive direction.
 $(\frac{\Delta P}{P_m})_{\max}^{-,o}$ is the maximum strength degradation of odd cycle in negative direction.

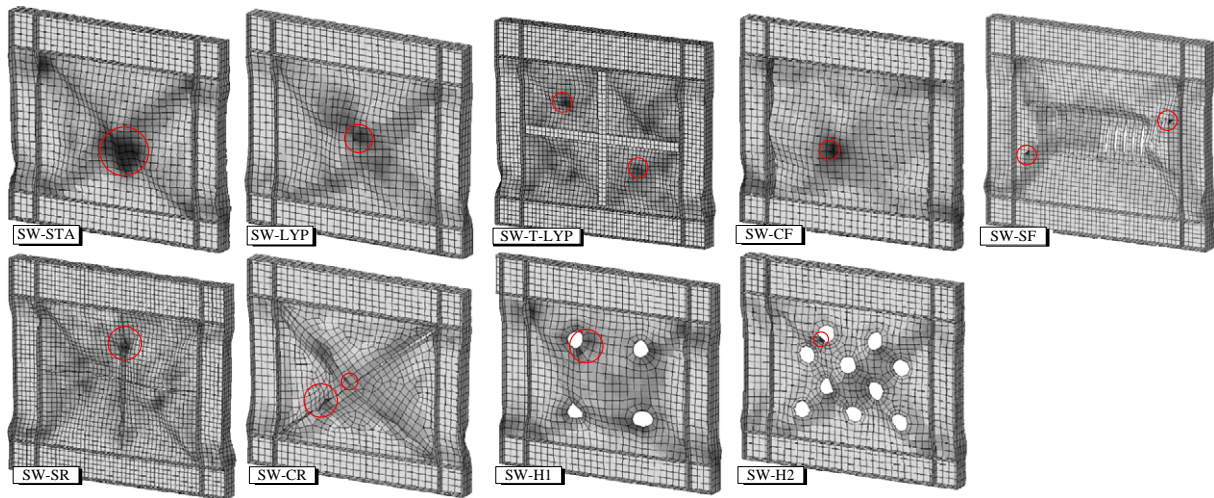


Fig. 20. Comparison of PEEQ distribution.

5.4. Comparison of fracture tendency

From the PEEQ distributions of structures in Fig. 20, the probable fracture and damage locations can be obtained. The construction details can change the deformation distributions and failure modes to improve the properties of shear wall structures. The points selected for fracture tendency PEEQ index comparisons include the middle position of shear plate (the effect of cyclic out-of-plane deformation on shear wall), the corner of shear plate (weld areas) and the center and edge of column flange (the effect of tension field on the columns) (Fig. 21). The PEEQ values of SW-SF, SW-SR, SW-CR, SW-LYP and SW-T-LYP in the middle of shear wall are higher than SW-STA, due to the stress concentration at ends of vertical slits, local buckling of stiffeners and deep yield stage of steel plate. However, the material ductility of low yield point steel is almost twice of normal steel, so the higher PEEQ value in steel plate of SW-LYP and SW-T-LYP may not lead to earlier fracture [16,17]. For SW-SR and SW-CR, the positions of maximum PEEQ are stiffeners, which could be treated as the first defense of shear wall structures. For SW-SF, the largest values are at the end of slits, which would lead to the infill steel panel torn at these positions. Except for SW-CR, the corner PEEQ values of the others are less than SW-STA, effectively lessening the fracture probability of welds around corners. The ductility of weld at root is much worse than base metal, usually causing brittle fracture and fatigue fail at welded joints (welded stiffener-to-web

panel joints) [29]. The plastic strain accumulation of SW-CR increases at the corners caused by the effect of both diagonal tension fields in steel plate and diagonal stiffeners, leading to larger PEEQ values. The PEEQ values of SW-CF, SW-LYP, SW-T-LYP, SW-H1, and SW-H2 at column flanges are less than SW-STA, indicating that these construction details reduce the adverse effects of tension fields on the columns. For the stiffened specimens of SW-SR and SW-CR, the effects of tension fields on the columns are increased, so higher demands of column stiffness are needed for structure design.

5.5. Comparison of failure modes

It can be seen from Fig. 22 that the details of holes, slits and stiffeners will change the deformation behaviors of thin steel plate shear walls, resulting in the changes of failure modes. During the loading process, the buckling of thin steel plate occurs early with the formation of tension strips and obvious out-of-plane deformations, leading to pinching phenomena of hysteretic curves. The maximum out-of-plane deformations of structures at 1/50 positions and final positions are compared in Table 7, in which the deformation of SW-T-LYP is the smallest, showing that the out-of-plane deformations are effectively restrained. One main wave is formed for SW-STA and SW-LYP with clear two-way tension strips. Due to the low yield point of material, the plate goes into yield state earlier, so there is little change during the loading

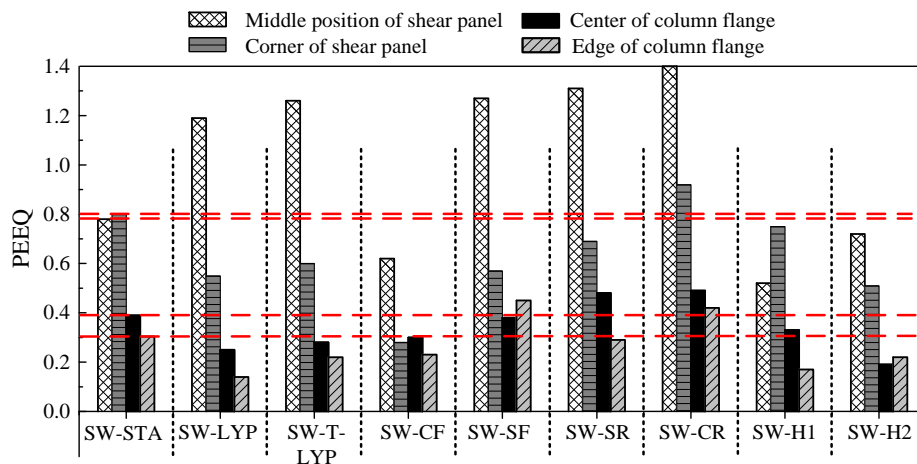


Fig. 21. Comparison of the maximum PEEQ.

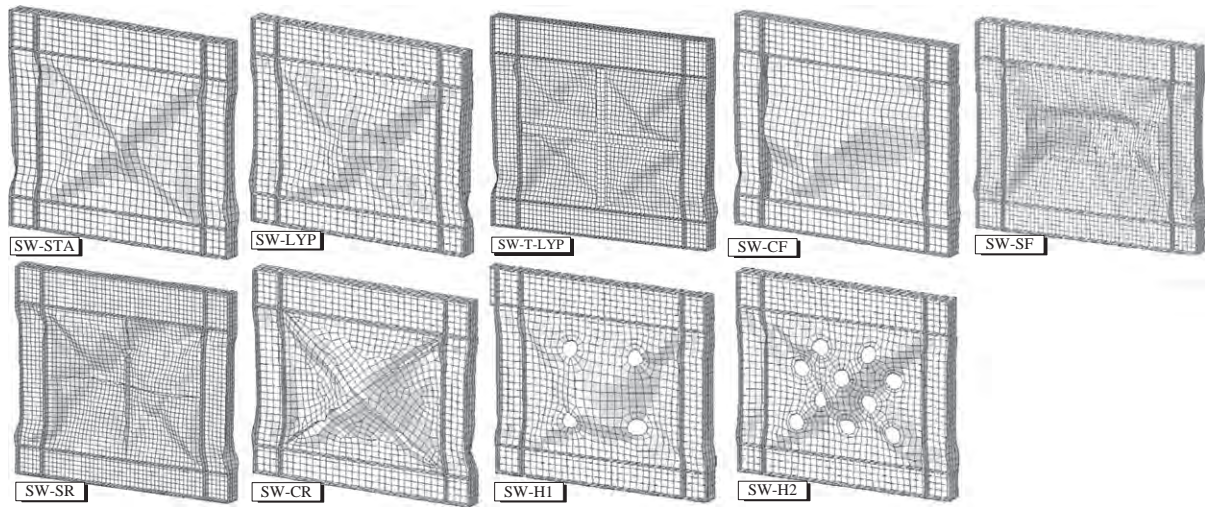


Fig. 22. Comparison of failure modes.

process. No clear tension strip of SW-CF is formed, and multi-wave bending failure mode is discovered. The failure modes of SW-SF are bending deformation of steel strips between slits with no significant main wave, lessening the out-of-plane deformation. For SW-SR, tension fields are formed in small stiffener compartments. Due to limited stiffness of stiffeners, the maximum deformation of SW-CR is at the intersection of stiffeners, forming a main wave failure mode. The panel deformations of SW-H1 and SW-H2 are averaged without obvious main waves, significantly reducing the out-of-plane deformation.

5.6. Comparison of energy dissipation capacity

The energy dissipation coefficient is one of the indices describing the energy dissipation capacity of components. The method to calculate energy dissipation coefficient is shown in Fig. 23 based on literature (JGJ101-96) [30]. In Eq. (5), S_{ABC} and S_{CDA} respectively refer to the upper half and lower half areas of the hysteresis curve; S_{OBE} and S_{ODF} respectively stand for the corresponding triangular areas. The larger the value of \bar{E} is, the stronger the energy dissipation capacity is.

$$\bar{E} = \frac{S_{(ABC+CDA)}}{S_{(OBE+ODF)}} \quad (5)$$

As the out-of-plane deformation of steel panels, a certain degree of pinching phenomena occurs in hysteresis curves, which affect the energy dissipation capacity of structures. Fig. 24(a)–(d) shows the changing trends of energy dissipation coefficient of all shear walls with the increasing distance between point E and point F in Fig. 23. From Fig. 24, the following characteristics of the steel plate shear wall energy dissipation can be obtained: 1) The energy dissipation coefficients increase with the increasing of displacements Δ_{EF} , indicating that the infill steel panels have better energy dissipation capacity. 2) The energy

dissipation capacity may be reduced subjected to the repeated loading under the same displacement, showing that the damage occurs under reciprocating loadings. 3) The occurrence of degradation may increase energy dissipation coefficient, because the hysteretic curves get plumper.

From the comparison of final energy dissipation coefficients in Fig. 24(e), the changes of structural forms will improve the energy dissipation capacity of the structure, in which the low yield point steel shear wall structures have the strongest energy dissipation capacity. The index of SW-LYP is higher than SW-SAT by nearly 12.4%, and the index of SW-T-LYP is higher than SW-SAT by nearly 16.4%.

5.7. Summary of the seismic behavior comparisons

In summary, the seismic behaviors of steel plate shear wall with different construction details are compared in Table 8. The appropriate details and materials can effectively change the deformation behavior, energy dissipation capacity, fracture properties, ductility and failure modes, and play a good role on improving the seismic performances of structures. Besides, they should be considered comprehensively with all kinds of performance. For example, the shear walls with slits improve the energy dissipation capacity and curve pinching problem and lessen the out-of-plane deformation and the impact of tension field on the columns, however, there is a significant reduction in strength and stiffness. The stiffened steel plate shear walls greatly improve the load-carrying capacity, however, the hysteretic curves still have significant pinching phenomena, due to the limited stiffness of stiffeners. The shear walls with openings change the failure modes, lessen the out-of-plane deformation and effectively reduce the influence of

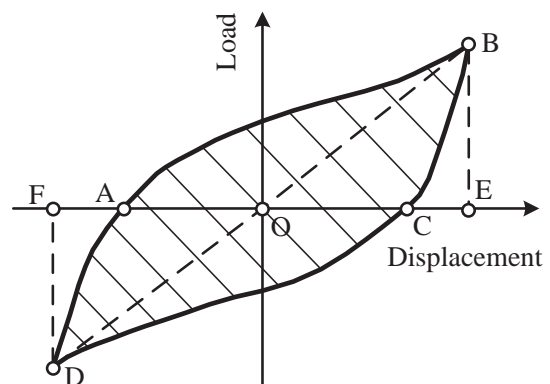


Fig. 23. Calculative method of energy dissipation coefficient.

Table 7
Comparison of out-of-plane deformations (mm).

Type	1/50 position	Final position
SW-STA	105.86	163.89
SW-LYP	139.82	159.17
SW-T-LYP	76.15	99.23
SW-CF	115.72	158.25
SW-SF	95.51	142.58
SW-SR	105.01	158.96
SW-CR	122.65	168.06
SW-H1	108.32	136.72
SW-H2	104.73	132.96

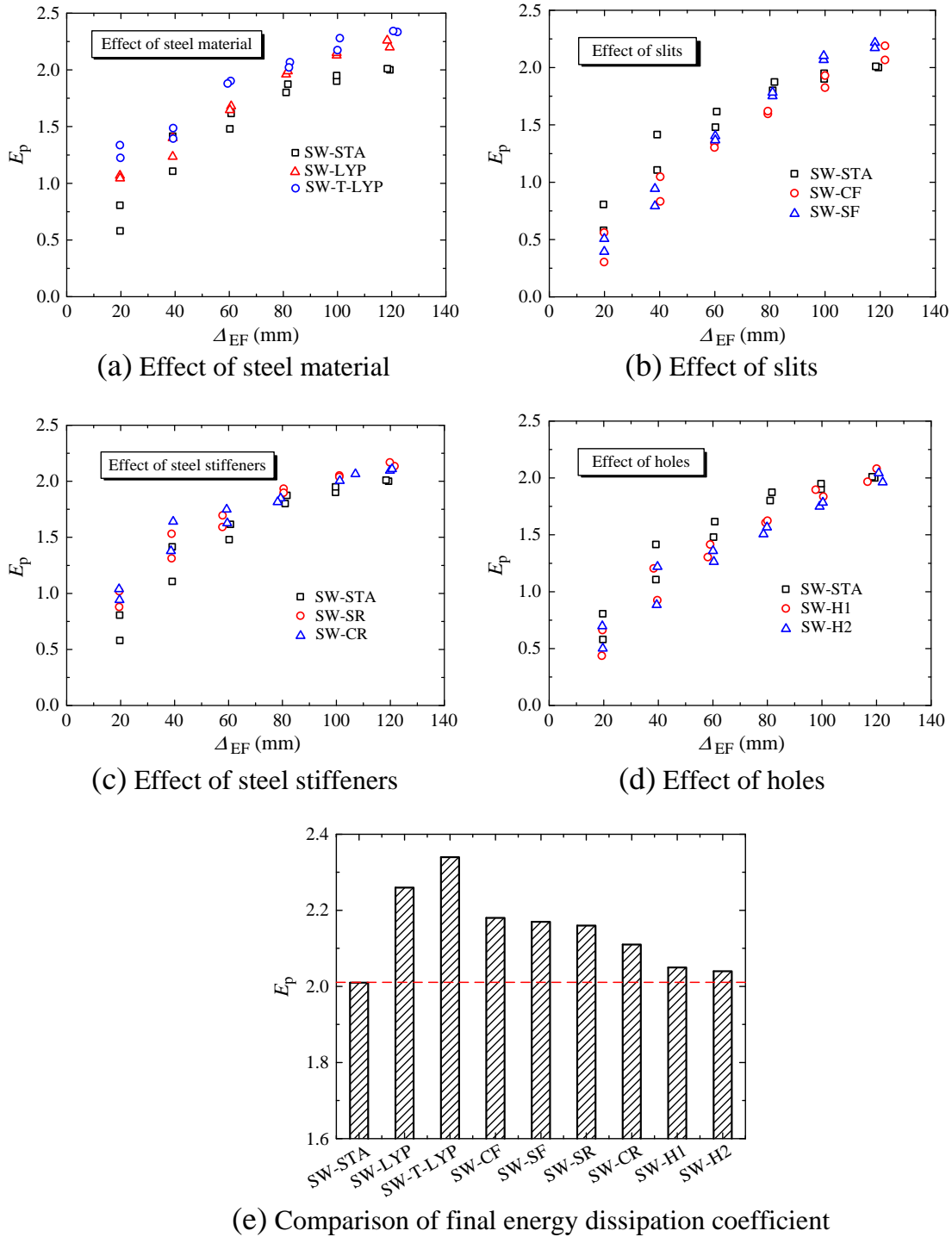


Fig. 24. Comparison of energy dissipation coefficient.

tension field on the columns, but the processing techniques are relatively complicated. The proposed T type rib stiffened low yield point steel plate shear wall can most effectively improve the energy dissipation capacity and ductility, and also lessen the impact of tension field on the columns.

6. Conclusions

The nonlinear finite element method of steel plate shear wall was established, which was verified by typical test results. Comparative

analyses of steel plate shear wall with different construction details were carried out. The following conclusions can be drawn:

- (1) The proposed finite element method could give a quite accurate prediction for behaviors of steel plate shear walls, including load-carrying capacity, hysteretic curves, failure modes and fracture tendencies. The rationality of selected element types and constitutive models and applications of initial defects are proved. The method provides a strong tool for studying the performances of steel plate shear walls.

Table 8
Comparison of seismic behaviors.

Type	Load-carrying capacity	Energy dissipation capacity	Fracture behavior of infill panel	Fracture behavior of the corner welds	The effect of tension field on the columns	Cumulative damage (ductility)	Failure mode	Economic performance
SW-STA	–	–	–	–	–	×	–	○
SW-LYP	△	○	△	○	○	○	△	○
SW-T-LYP	○	○	△	○	○	○	○	△
SW-CF	△	△	○	○	○	○	△	○
SW-SF	×	△	×	○	△	△	○	△
SW-SR	○	△	×	△	×	×	△	△
SW-CR	○	△	×	×	×	×	×	△
SW-H1	○	△	○	△	△	△	○	△
SW-H2	○	△	○	○	○	△	○	△

Note: ○ Good; △ Medium; × Poor.

- (2) The appropriate construction details of steel plate shear wall structures can effectively improve the seismic performance of structures, including the deformation behavior, energy dissipation capacity, fracture properties, ductility and failure modes. For example, SW-CR and SW-SR can increase the load-carrying capacity of structures. The hysteretic loops of SW-SF, SW-CF, SW-LYP, and SW-T-LYP are plumper with less pinching phenomena and better energy dissipation capacity. The strength degradations of SW-LYP, SW-T-LYP, SW-CF, SW-SF SW-H1 and SW-H2 are less than 15% at 1/50 position with good ductility. The out-of-plane deformations of SW-T-LYP, SW-SF, SW-H1 and SW-H2 are effectively lessened. SW-CF, SW-T-LYP, SW-LYP, SW-H1 and SW-H2 reduce the adverse effects of tension fields on the columns.
- (3) In the high seismic zones, according to the specific demands of actual projects, load-carrying capacity, hysteretic behaviors, failure modes, seismic ductility and economic performance should be all taken into account comprehensively to choose appropriate constructions of shear walls. From the seismic behavior comparison of steel plate shear walls with different constructions, the proposed T type rib stiffened low yield point steel plate shear wall can most effectively improve the energy dissipation capacity and ductility, and also lessen the impact of tension field on the columns. Besides, it has better load-carrying capacity and smallest out-of-plane deformation. This method achieves the combination of high-performance structural form and high-performance material, and provides a good way for improving the seismic behaviors of steel shear wall structures.

Acknowledgments

This work described in paper was supported by the National Natural Science Foundation Grant (No. 51408031), Beijing Natural Science Foundation (No. 8154052), China Postdoctoral Science Foundation Grant (2014M550021) and Fundamental Research Funds of Central Universities (2014JBM074).

References

- Guo YL, Dong QL. Research and application of steel plate shear wall in high-rise buildings. *Steel Constr* 2005;25(1):1–6.
- Chen GD. The investigation to structural behavior of steel plate shear walls. [Doctoral dissertation] Beijing, China: Tsinghua University; 2002.
- Vian D, Bruneau M, Tsai KC, Lin YC. Special perforated steel plate shear walls with reduced beam section anchor beams. I: experimental investigation. *J Struct Eng* 2009;135(3):211–20.
- Wang L. The investigation to structural behavior of perforated steel shear walls. [Doctoral dissertation] Xian, China: Xian University of Architecture and Technology; 2009.
- Guo YL, Miu Y w, Dong LQ. Elastic buckling behavior of stiffened steel plate shear walls slotted at two edges. *Prog Steel Build Struct* 2007;9(3):58–62.
- Hitaka T, Matsui C. Experimental of study on shear wall with slits. *J Struct Eng* 2003;129(5):586–95.
- Chen YY, Ning YQ, Jiang L. Experimental study on seismic behavior of frame-steel plate shear wall with slits. *J Build Struct* 2012;33(7):133–9.
- Li F. Experimental and theoretical investigation to earthquake resistant behavior of steel plate shear wall. [Doctoral dissertation] Xian, China: Xian University of Architecture and Technology; 2011.
- Alavi E, Nateghi F. Experimental study of diagonally stiffened steel plate shear walls. *J Struct Eng* 2013;139(11):1795–811.
- Alinia MM, Dastfan M. Cyclic behavior, deformability and rigidity of stiffened steel shear panels. *J Constr Steel Res* 2007;63(4):554–63.
- Li F, Li H, Li ZM, Li ZJ, Chen XF, Ding L. Cyclic test of diagonally stiffened steel plate shear wall. *J Xian Univ Architect Technol (Nat Sci Ed)* 2009;41(1):57–62.
- Dong LQ. Studies on structural behavior and design method of buckling-restrained steel plate shear wall. [Doctoral dissertation] Beijing, China: Tsinghua University; 2007.
- Chen SJ, Jhang C. Cyclic behavior of low yield point steel shear walls. *Thin-Walled Struct* 2006;44(7):730–8.
- Chen SJ, Jhang C. Experimental study of low-yield-point steel plate shear wall under in-plane load. *J Constr Steel Res* 2011;67(6):977–85.
- Nakashima M, Iwai S, Iwata M, et al. Energy dissipation behavior of shear panels made of low yield steel. *Earthq Eng Struct Dyn* 1994;23(12):1299–313.
- Nakashima M. Strain-hardening behavior of shear panels made of low-yield steel I: test. *J Struct Eng ASCE* 1995;121(12):1742–9.
- Nakashima M, Akawaza T, Tsuji B. Strain-hardening behavior of shear panels made of low-yield steel II: model. *J Struct Eng ASCE* 1995;121(12):1750–7.
- Shi YJ, Wang M, Wang YQ. Experimental and constitutive model study of structural steel under cyclic loading. *J Constr Steel Res* 2011;67(8):1185–97.
- Driver RG, Kulak GL, Kennedy DJL, Elwi AE. Seismic behavior of steel plate shear walls. *Structural Engineering, Rep. No., 215. Dept. of Civil and Environmental Engineering, University of Alberta*; 1997.
- Wang M. Damage and degradation behaviors of steel frames under severe earthquake. [Doctoral dissertation] Beijing: Tsinghua University; 2013.
- Chaboche JL. Time independent constitutive theories for cyclic plasticity. *Int J Plast* 1986;2(2):149–88.
- Chaboche JL. Constitutive equations for cyclic plasticity and cyclic viscoplasticity. *Int J Plast* 1989;5(3):247–302.
- ABAQUS. Analysis user's manual IV. Version 6.10. USA: ABAQUS, Inc., Dassault Systèmes; 2010.
- Xu Jian. Research on the behavior and design methods of unstiffened thin steel plate shear wall. [Doctoral dissertation] Chongqing, China: Chongqing University; 2012.
- Canadian Standards Association. CAN/CSA-S16-01. Limits states design of steel structures. Canada: Standards Council of Canada; 2001.
- AISC Committee. ANSI/AISC 341-05. Seismic provisions for structural steel buildings. America: American Institute of Steel Construction; 2005.
- Peter D, Ahmad MI, Ian GB. Cyclic response of plate steels under large inelastic strains. *J Constr Steel Res* 2007;63(2):156–64.
- Ministry of Housing and Urban-Rural Development of the People's Republic of China. GB50011-2001 code for seismic design of buildings. Beijing: China Architecture & Building Press; 2001.
- Shi G, Wang M, Wang YQ, Wang Fei. Cyclic behavior of 460 MPa high strength structural steel and welded connection under earthquake loading. *Adv Struct Eng* 2013;16(3):451–66.
- Ministry of Housing and Urban-Rural Development of the People's Republic of China. JGJ101-96 specification of testing methods for earthquake resistant building. Beijing, China: Architecture & Building Press; 1997.